Pure Appl. Chem., Vol. 85, No. 1, pp. 247–256, 2013.
http://dx.doi.org/10.1351/PAC-CON-12-02-01

Cellular automata approach to corrosion and passivity phenomena*

Łukasz Bartosik[1], Dung di Caprio[2], and Janusz Stafiej[1,‡]

[1]Institute of Physical Chemistry, Polish Academy of Sciences, Kasprzaka 44/52, 01-224 Warsaw, Poland; [2]LECIME, l'ENSCP, UMR 7575 du CNRS, 4. Place Jussieu, 75005 Paris, France

Abstract: Our research on employing the cellular automata methodology to corrosion and passivation phenomena is reviewed. Examples of a peculiar pit development are found and presented. The diffusion rate in the corroding medium is argued and shown in the simulation results to affect mainly the characteristic length scale for the corrosion process. New data for the pitting corrosion development on a planar interface are presented and discussed.

Keywords: computer modeling; computer simulation; corrosion; interfaces; nanomaterials; passivation; surface chemistry.

INTRODUCTION

Corrosion and passivation phenomena are old and venerable subject areas, combining the coupling of the solution chemistry of the environment with the interfacial phenomena of the metal surface exposed to this environment [1]. Because of the huge economic importance of corrosion protection [2], there have been numerous studies on the stability of the passive layer mainly on the experimental side [3,4]. However, a recent renewed interest in the passive layer functioning arises also from their potential application in nanotechnology and nanoengineering. The spontaneous organization of nanopores in oxide layers on anodized metal surfaces is an example of such potential applications [5,6]. This is related to the fact that passivating metal solutions can exhibit complicated oscillatory behaviors both in space and time observed experimentally [7,8]. This in turn is a strong challenge for a theoretical description and raises many questions on how to elaborate a unified approach that would cover various aspects of corrosion and passivation, such as generalized corrosion as opposed to localized pit nucleation and development, eventual pit healing, passive layer morphology, and the existence of various morphological regimes of the passive layer depending on the physicochemical conditions of its formation. The latter leads immediately to the particular question: How does it occur that the layer morphology can be that of an ordered hexagonal lattice of pores of fairly well-defined sizes on the mesoscopic scale?

In this paper, we show our first attempts to address those questions. The first problem we encounter on this way is the choice of the method and particularly the level of description. Is it possible to use atomic- or molecular-level simulations of the Monte Carlo or molecular dynamics type? We really doubt that it is possible or expedient for the problems posed above. For instance, pit nucleation is a rather scarce event on the atomistic scale. The nanopores form with the size of the order of magnitude in the range 10–100 nm. Then the time and space scales of the phenomena are far beyond the reach

Pure Appl. Chem.* **85, 1–305 (2013). A collection of invited papers based on presentations at the 32nd International Conference on Solution Chemistry (ICSC-32), La Grande Motte, France, 28 August–2 September 2011.
‡Corresponding author

of the present-day atomistic level computations. On the other extreme, we can consider a macroscopic description with classical kinetic equations. It is known, however, that such descriptions can be rather inaccurate. For instance, they fail to predict the separation of reagents in annihilation reaction A + B $\rightarrow$ 0 in 2D or 1D confirmed both by simulation and experiments in limited quasi-1D or 2D geometry [9,10]. Thus, their use may overlook important qualitative features of the phenomena. Additionally, in most cases we do not have analytical solutions of the resulting equations and we are obliged to use some kind of discretization to be able to solve the problem numerically.

Thus, we decide to work on the mesoscopic level using a cellular automata discretized approach right from the beginning. The archetype of such an approach is the theory of Brownian motion that combines macroscopic physics—viscosity and Stokes formula for the viscous friction of the spherical object with stochastic noise coming from the microscopic physics. In a cellular automata approach, Brownian motion is represented by a random walk over the lattice [11].

Invented by John von Neumann, the father of the first computers, and the mathematician S. Ułam [12,13], cellular automata have been successfully applied in a wide range of fields: biology [14–16], traffic jams [17,18], fire spreading [19], lava eruption [20], urban development [21], and a variety of growth problems [22]. Their application to corrosion problems also has a fairly long history [23,24]. In this paper, we reconsider our own contribution [25–29] to show the methods and lines of thinking that led us to an attempt at using cellular automata to model corrosion on passivating metal surfaces. Besides the mere elimination, neither micro- nor macroscopic descriptions are suited for our purposes, the argument to support our choice is that the phenomena we want to understand are rather general. Passivation is the reason for relative (meta)stability of most metals and alloys of practical use. The hexagonally organized nanopore formation is most studied and documented on the aluminum surface [5,6,30], but in recent years the phenomenon has been experimentally documented for many other metal surfaces largely different from aluminum with respect to the metal electronic structure and metal chemical reactivity [30]. Thus, the phenomenon does not depend crucially on the details of microscopic description of the given metal and we can use a simpler description based on general physics.

In this paper, we concentrate mainly on our model for anodic and cathodic zone separation [25–27] for the corrosion in view of a considerable interest in this subject [31,32]. We show how a characteristic length appears in this model and present some so far unpublished results on the surface development and pit generation. Then we briefly review our recent models on passivation phenomena [28,29] and discuss how we intend to adapt those models for nanopore formation modeling.

CATHODIC AND ANODIC ZONE SEPARATION

The model for cathodic and anodic zone separation has been already presented in several papers [25–27] in the following context. The metal surface is covered by an insulating layer, for instance, a paint. A small isolated damage in this paint layer initiates a corrosion process. The role of the paint is twofold. First, it imposes a particular point-like geometry from which the corrosion may start. Second, it imposes the open circuit condition on the developing pit. Then we describe the evolution of this process. In the following section, we briefly recollect the physicochemical basis of the model here and its cellular automata realization, and we describe the main results. In addition, we present the results of this model in a different problem where initially the whole surface is exposed to the aggressive environment.

Model description

Physicochemical basis

The anodic metal dissolution

$$\mathrm{Me} \rightarrow \mathrm{Me}^{+}_{\mathrm{aq}} + e^{-} \tag{1}$$

is followed by metal cation hydrolysis

$$Me^{+}_{aq} + H_2O \rightarrow MeOH_{aq} + H^{+} \quad (2)$$

which creates an acidified environment at the site where it occurs. In addition, anions have to be moved to this locality to preserve electroneutrality, creating an overall aggressive environment that promotes solubilization of the passive layer and impedes repassivation. The cathodic reaction in deaerated solution reduces the local acidity by hydrogen evolution

$$H^{+} + e^{-} \rightarrow \tfrac{1}{2}H_2 \quad (3)$$

$$H_2O + e^{-} \rightarrow \tfrac{1}{2}H_2 + OH^{-} \quad (4)$$

The metal surface mediates in the electron exchange. The more basic environment thus created in general is more favorable for passivation and much less harmful to the passive layer than the environment created by anodic reaction. In the basic environment, the anodic reaction may take the form of repassivation, leaving the product adherent to the surface

$$Me + OH^{-} \rightarrow MeOH_{ads} + e^{-} \quad (5)$$

In the acidic environment, the adsorbed hydroxides (and oxides) adherent to the metal surface are likely to detach by inverse hydrolysis.

$$MeOH_{ads} + H^{+} \rightarrow Me^{+}_{aq} + H_2O \rightarrow MeOH_{aq} + H^{+} \quad (6)$$

The cathodic and anodic solutions mutually neutralize, restoring the pH of the initial solution.

$$H^{+} + OH^{-} \rightarrow H_2O \quad (7)$$

Cellular automata coding

Cellular automata system

In the cellular automata spirit the system considered consists of a network of discrete sites corresponding to given spacial locations and often organized in a symmetrical fashion as a lattice with given connectivity rules. Here we use the square lattice with von Neumann and Moore connectivities in two dimensions. According to the predominant chemical composition at the site location, the site can be found in seven states or, as it is said in physical chemistry, can be occupied by seven species denoted M, R, P, E, A, B, and W. M stands for bulk metal, R and P denote surface metal sites that can be either reactive R or passive P. E labels those sites of the metal environment that have the properties of the initial solution unchanged by the corrosion process, A denotes acidic sites formed in anodic metal dissolution, while B denotes basic sites formed by a cathodic decomposition of water. Finally, W or wall sites are introduced to imitate the presence of the neutral paint or impose the boundaries of the system as they remain unchanged during the system evolution.

Dynamic rules

These rules give the state of the system at a given time step based on the state of the system in the precedent time step. We do not require that these rules are local as we represent a system with coulombic interaction where the information on electric state of the system spreads very fast compared to other processes. The rules are so devised as to mimic, as closely as possible, the physicochemical processes mentioned above on a mesoscopic level.

The first most trivial rule has already been stated for the W sites

$$W \rightarrow W \quad (8)$$

independent of any circumstances.

The reactive sites can undergo anodic dissolution according to the scheme

$$R \rightarrow A \quad (9)$$

in acidic and neutral solution around them and

$$R + B(nn) \rightarrow P + E(nn) \tag{10}$$

in basic environment. Here, B(nn) and then E(nn) are nearest-neighbor sites of the site R that can change type to become a P site after transformation. The anodic dissolution can undergo only together with a cathodic reaction. From among all surface sites connected to the site R, one site S either of type R or P is selected at random and tested for the reactions

$$S + E(nn) \rightarrow S + B(nn) \tag{11}$$

or

$$S + A(nn) \rightarrow S + E(nn) \tag{12}$$

Thus, the anodic dissolution is dependent on the existence of a single, maybe remote site that is not blocked by B sites. In practice, it is not very restrictive for a sufficiently large system. In theory, however, it makes all the connected sites interdependent where connectivity means the existence of a chain of nearest neighbors of sites M, R, or P that form a path between the two sites. This ensures the electronic transfer between anodic and cathodic sites. This obliges us to keep and update the information on metal connectivity during the simulation, which is a tricky and time-consuming part of the simulation algorithm.

Other rules are local. They represent local dissolution of R and P sites

$$R \rightarrow E \tag{13}$$

and

$$P \rightarrow E \tag{14}$$

and repassivation

$$R \rightarrow P \tag{15}$$

Finally, we assume simple exclusion random walk of A and B sites created in spatially separated electrochemical reactions and their mutual annihilation if A steps on B or vice versa. It can be formally expressed as

$$A + E \rightarrow E + A \tag{16}$$

$$B + E \rightarrow E + B \tag{17}$$

$$A + B \rightarrow E + E \tag{18}$$

$$B + A \rightarrow E + E \tag{19}$$

$$A + X \rightarrow A + X \text{ for } X \neq B \text{ and } X \neq E \tag{20}$$

$$B + X \rightarrow B + X \text{ for } X \neq A \text{ and } X \neq E \tag{21}$$

When A and B sites step on an E site, they swap with the E site. When A attempts to step on B or vice versa, both turn into E sites. Nothing happens for all other cases.

Model parameters

The principal model parameters are the arbitrarily set time and length scales for discrete lattice constant a and time step dt. Then we have probabilities or the rates of the processes 9–21 that can be recalculated to the real world units using a and dt. We assume a single value P_{SSE} for the probability of occurrence of the spatially separated anodic (processes 9 and 10) and cathodic (processes 11 and 12) reactions. Probabilities related to processes 13–15 are denoted P_{RE}, P_{PE}, P_{RP}, respectively. We describe

their dependence on the local acidity/basicity using the excess of A sites over B sites $N^{exc}{}_{nn}$ in the following way:

If $N^{exc}{}_{nn} > 0$, then

$$P_{RE} = p_{cor2}\, N^{exc}{}_{nn} \text{ and } P_{PE} = 0.25\, N^{exc}{}_{nn} \text{ and } P_{RP} = 0 \quad (22)$$

if $N^{exc}{}_{nn} = 0$, then

$$P_{RE} = 0 \text{ and } P_{PE} = p_{oxi} \text{ and } P_{RP} = p_{cor1} \quad (23)$$

if $N^{exc}{}_{nn} < 0$, then

$$P_{RE} = P_{PE} = 0 \text{ and } P_{RP} = 1 \quad (24)$$

Equations 22–24 correspond to acidic, neutral, and basic environment, respectively. In a rough way, they introduce the known phenomenology discussed in the section "Physicochemical basis". The constant parameters p_{cor1}, p_{cor2} can be set as a first guess to 0. In contrast, p_{oxi} cannot be 0. Otherwise, depassivation would never occur and the onset of the electrochemical dissolution according to eqs. 9 and 10 would not be possible.

Finally, there are the rates of random walk and annihilation. We assume that diffusion rates of A and B species are equal and each of them is given N_{diff} chances to execute a random walk step in one simulation time step. When the site to walk gets its chance, its nearest neighbor is selected at random. If the neighbor is an E site, the swap of eqs. 16 and 17 is executed with certainty. If it is the opposite site (B for A and A for B), the annihilation of eqs. 18 and 19 is also executed with certainty. These are our arbitrary selections to keep the problem most simple and the number of parameters as small as possible. These selections can be modified if needed in a future work.

The size of the simulation box for the data presented here is always 1000×1000. For the single cavity evolution, the initial condition is a block of metal 998×998 sites surrounded by wall sites at left-, right-, upper-, and lowermost site layers. The layer damage is simulated by turning the metal sites 500 and 501 in the middle of the uppermost metal layer to passive sites and assuming they are subject to the above-described rules of evolution from now on as in contact with the aggressive solution. For the planar interface, the initial condition is the lower half of the box filled with metal covered by a layer of passive sites and then the solution fills the rest of the box. Periodic boundary conditions are applied parallel to this initial surface.

RESULTS AND DISCUSSION

Evolution of point-like damage

Most of the results for the evolution of the point-like damage have already been presented and discussed in our earlier papers. The general image that can be drawn from these papers is the following. Despite the various parameters in the model, the evolution of the damage has just one scenario with two subvariants. In the beginning, when the diffusion is fast enough to bring about homogeneity and neutralization, the development of the damage is rather symmetrical and semicircular in shape until the size of the cavity reaches a critical value. Then we deal with all kinds of peculiar shape variations related to the appearance of anodic and cathodic zones and the spontaneous symmetry breaking where some initial pH fluctuations on a small scale get amplified to the specific scale of the transition. When the cavity grows larger than this scale, the roughly homogeneous semicircular growth pattern is restored with decorations on the periphery of the circle. The decorations retain the scale of the symmetry-breaking patterns. The zone separation is accompanied by the change in the corrosion rate. Normally, when the anodic dissolution rate is comparable to depassivation rate the appearance of zones increases the corrosion rate as the appearance of the zones increases the metal surface exposed to anodic environment. When anodic corrosion is very fast then soon the majority of the surface is exposed to anodic environ-

ment. Development of the cathodic zones reduces that area, and hence the appearance of zone separation slows down the process.

We should like to present some further results here. First, an example of a peculiar-shaped cavity development is presented in Fig. 1. The damage initiating the corrosion is positioned in the middle of the top part of the layer protecting a square piece of the metal. The cavity starts developing bottom-wise in a fairly symmetrical fashion. Then the zone arrangement appearing in the course of simulation results in an asymmetrical development of an anodic part of the cavity that finally touches the boundaries of the square. This type of development suggests a possible mechanism of lacy cover development in 3D in which the initial pit entry is surrounded by holes resulting from the development of the pit upwards, arriving at the metal surface [33].

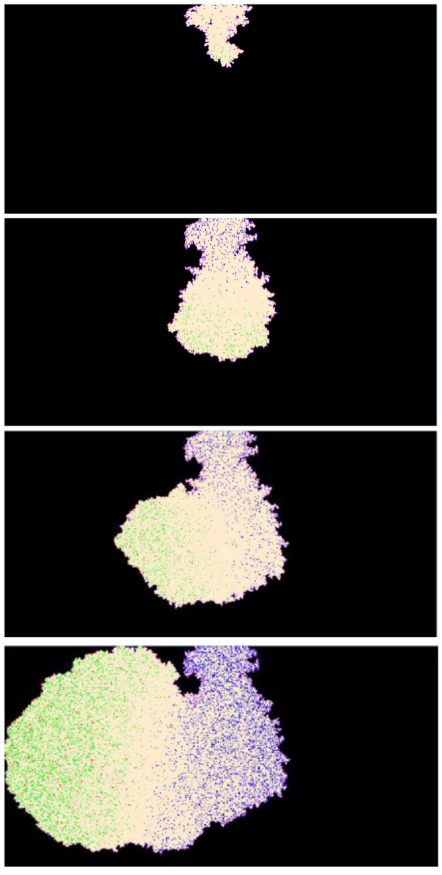

Fig. 1 Example of a peculiar cavity development. The snapshots correspond to N_t = 4500, 6500, 7000, 7679 time steps. $p_{oxi} = 10^{-3}$, $p_{cor1} = p_{cor2} = 0$, $p_{SSE} = 0.5$. The color codes (online version) are as follows: E – light beige, M – black, R – red, P – violet, A – light green, B – dark blue. In the gray scale (print version) where 0 and 1 correspond to black and white, respectively, the site codes are: E – 0.70, M – 0.00, R – 0.80, P – 0.20, A – 0.95, B – 0.5.

The dependence of the equivalent cavity radius on the simulation time step shown in Fig. 2 allows us to make a rough estimate of the transition time as about N_t = 5000 time steps. We can notice that the cavity shape is fairly asymmetrical and irregular prior to the transition. We will return to this point later on.

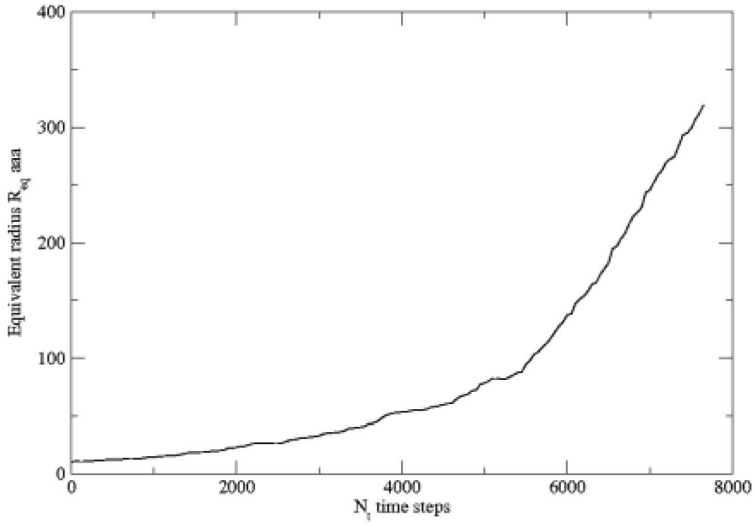

Fig. 2 The dependence of the equivalent cavity radius R_{eq} on simulation time step N_t. $R_{eq} = (2S/\pi)^{1/2}$ where S is the cavity area.

It is interesting to see the effect of diffusion on the cavity development within our limited simulation box size and simulation time. In Fig. 3, we present a series of results with N_{diff} ranging from 1 to 10^5.

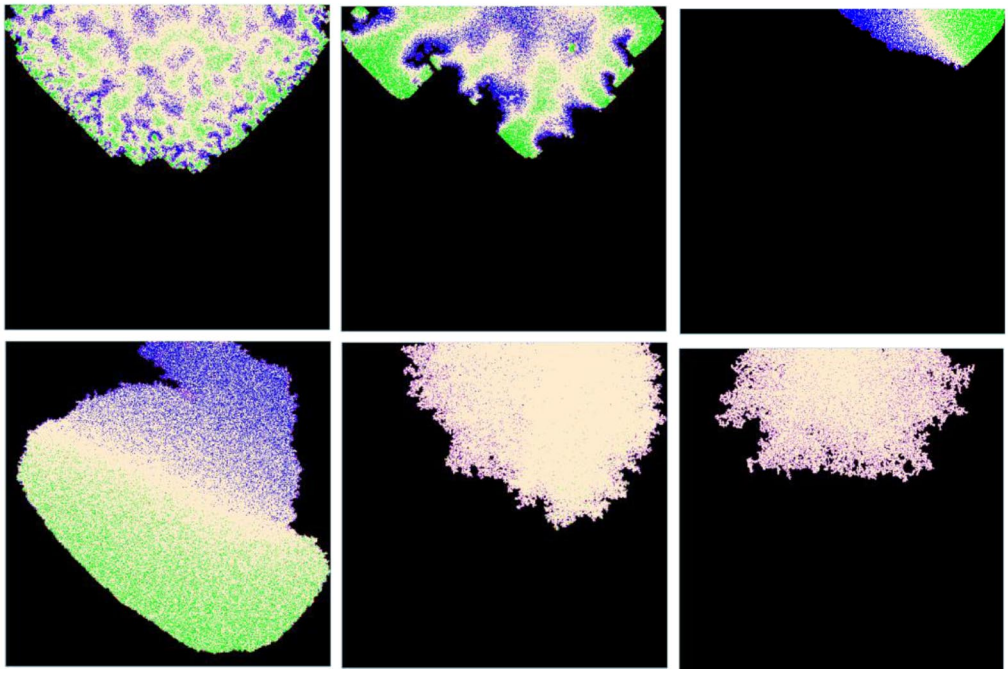

Fig. 3 The cavity shape on the length scale of the simulation box for various rates of diffusion, N_{diff} = 1, 10, 100, 10^3, 10^4, 10^5 from top left to bottom right snapshot at the time steps N_t = 636, 613, 638, 1925, 3353, and 3849, respectively, $p_{oxi} = 10^{-3}$, $p_{cor1} = p_{cor2} = 0$, $p_{SSE} = 1$.

Let us note that the length scale of the anodic and cathodic zones increases so that we do not observe them any more for $N_{diff} = 10^4$. However, an asymmetric cavity shape suggests some zone separation starting to form. For $N_{diff} = 10^5$, the shape is roughly symmetric with dental-like pit structure that differs largely from the almost semicircular cavities presented elsewhere. Those dental-like structures come from the fact that depassivated places on the surface susceptible to anodic dissolution survive relatively long especially when cached in pores in the metal and hidden from the impact of neutralization brought about by faster diffusion of basic cathodic sites. The porous structure formed reduces effectively the local diffusion coefficient favoring the survival of small anodic pits.

Evolution of planar interface

The main feature in the evolution of the planar interface is the formation of corrosion pits as presented in Fig. 4.

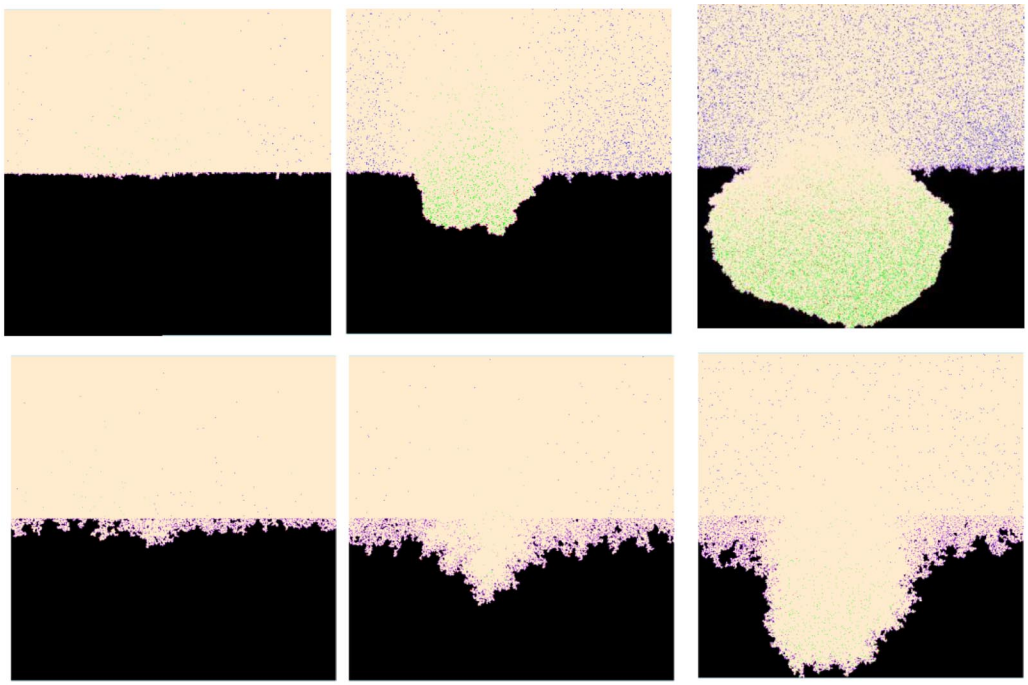

Fig. 4 Two examples of anodic pit formation. The first row contains snapshots for $N_t = 500, 1500, 2357$ from left to right, respectively, $p_{SSE} = 0.5$ and $N_{diff} = 1000$. The second row contains snapshots for $N_t = 500, 1000, 1557$, $p_{SSE} = 1$, and $N_{diff} = 10000$. In both cases, $p_{oxi} = 10^{-3}$, $p_{cor1} = p_{cor2} = 0$.

It follows that our toy model for the simulation of corrosion process reproduces the main features of real corrosion processes. The pits formed are filled up with anodic acidic solution while the outer space serves as a cathode and tends to be protected.

The pit formation here is a symmetry-breaking process arising spontaneously from fluctuations in the local composition of the solution close to the surface. The fluctuations are coupled to the surface reaction by an autocatalytic mechanism that may amplify their effect. In real systems, pit nucleation is often caused by local heterogeneities, for instance, inclusions that more readily initiate and sustain the pit growth than random fluctuations [34]. But in a large time scale, large surface areas and ill-controlled conditions are a possible cause of spontaneous pit initiation and as such must be considered.

The evolution shown in the second row of Fig. 4 is illustrative for a possible multiscale character of the pitting corrosion. On one hand we see a surface with many individual, apparently metastable pits on a smaller length scale. The large, "macroscopic", pit development is kind of superimposed on this structure. Clearly, we deal with multiscale phenomena where the concept of a scale-free fractal is not adequate. Where do the length scales in our model come from? Certainly this cannot be the lattice constant. As arbitrarily selected, it should not be relevant for the problem. On the macroscopic level, the model is characterized by the diffusion coefficient D and the rate constants k_i related to N_{diff} and heterogenous reaction event probabilities discussed above. Their dimensions are $[D] = \mathrm{L}^2\mathrm{T}^{-1}$ and $[k_i] = \mathrm{LT}^{-1}$ length squared per time and length per time respectively. Thus, the ratios $[D/k_i] = \mathrm{L}$ have the wanted dimension of length. This explains why changing N_{diff} seems to affect primarily the length scale of the system, although we may ignore the precise form of this dependence.

CONCLUSIONS

The ratio D/k_i proves useful in other contexts. We can recognize it in the expression for the cross-over cavity radius from slower to faster corrosion where k_i is the metal dissolution velocity in acidified medium [26]. Such a ratio directly gives the thickness of passive layer dissolution at the cross-over from reaction-controlled regime to diffusion-controlled regime [35,36]. Here we concentrated mainly on the effect of zone separation and reduced the passive layer thickness to the scale under the arbitrary lattice constant, practically zero. In papers [35,36], this thickness is asymptotically infinite. In more recent papers, we attempt to overcome the simplifications [35,36] and construct a realistic model of the passive layer with a finite thickness [28,29]. There seems to be a whole new world of problems, different structures and behaviors to discover that cannot be treated with quasi-1D classical approaches. We show that even in our primitive approach the passive layer can function in a very subtle way. If the layer material adheres well to the metal surface, a thin passive layer forms at the passivation transition that is enough to build up a protection [29]. If there is no adherence, the system compensates by a build-up of a thicker layer [28] so the protection is similar, however, the structure is quite different.

It is natural to think about a model that would combine a realistic description of the passive layer with the zone separation and other effects that may arise due to a slow diffusion rate, for instance, within the passive layer material. We have already shown preliminary results of our work in this direction for the problem of nanopore formation on anodized metal surfaces [37]. The primary goal is to master the parallel computing to be able to overcome the computation limitation that has forced us to work with 2D systems.

ACKNOWLEDGMENTS

The work presented here is done within the Polish Ministry of Science and Superior Education Grant No. N N204 139 038 administered by National Science Center. This work is also done as a part of the Ph.D. thesis completion of one of us (Ł. Bartosik) under fellowship of the Foundation for the Polish Science project B8.

REFERENCES

1. H. H. Uhlig. *Corros. Sci.* **19**, 777 (1979).
2. D. Landoldt. *Corrosion et Chimie de Surfaces des Metaux*, Presses Polytechniques et Universitaires Romandes, Lausanne (1993).
3. Z. Szklarska-Smialowska. *Corros. Sci.* **44**, 1143 (2002).
4. Z. Szklarska-Smialowska. *Pitting and Crevice Corrosion*, NACE International, Houston (2005).
5. R. C. Furneaux, W. R. Rigby, A. P. Davidson. *Nature* **337**, 147 (1989).
6. G. Cao, D. Liu. *Adv. Colloid Interface Sci.* **136**, 45 (2008).

7. D. Sazou, M. Pagitsas. *Chaos, Solitons Fractals* **17**, 505 (2003).
8. M. Pagitsas, A. Diamantopoulou, D. Sazou. *Electrochem. Commun*. **3**, 330 (2001).
9. K. Lindenberg, P. Argyrakis, R. Kopelman. *J. Phys. Chem.* **98**, 3389 (1997).
10. P. Argyrakis, R. Kopelman. *Phys. Rev. E* **47**, 3757 (1993).
11. R. H. Landau, M. J. Paez, C. C. Bordeianu. *Computational Physics. Problem Solving with Computers*, pp. 145–147, Wiley-VCH (2007).
12. J. von Neumann. *Theory of Self-Reproducing Automata*, edited and completed by A. W. Burks, University of Illinois Press, Urbana (1966).
13. W. Aspray. *John Von Neumann and the Origins of Modern Computing*, The MIT Press, Cambridge, MA (1990).
14. Y. Lee, S. Kouvroukoglou, L. McIntire, K. Zygourakis. *Biophys. J.* **69**, 1284 (1995).
15. J. W. T. Wimpenny, R. Colasanti. *FEMS Microb. Ecol.* **22**, 1 (2006).
16. G. G. Lazareva, V. V. Mironova, N. A. Omelyanchuk, I. V. Shvab, V. A. Vshivkov, D. N. Gorpinchenko, S. V. Nikolaev, N. A. Kolchanov. *Numer. Anal. Appl.* **1**, 123 (2008).
17. D. Chowdhury, L. Santen, A. Schadschneider. *Phys. Rep.* **329**, 199 (2000).
18. M. J. Kearney. *Phys. Rev. E* **74**, 061115 (2006).
19. A. Hernández Encinas, L. Hernández Encinas, S. Hoya White, A. Martín del Rey, G. Rodríguez Sánchez. *Adv. Eng. Software* **38**, 372 (2007).
20. G. M. Crisci, M. V. Avolio, B. Behncke, D. D'Ambrosio, S. Di Gregorio, V. Lupiano, M. Neri, R. Rongo, W. Spataro. *J. Geophys. Res*. **115**, 1 (2010).
21. D. P. Ward, A. T. Murray, S. R. Phinn. *Comput. Environ. Urban Syst.* **24**, 539 (2000).
22. A.-L. Barabási, H. E. Stanley. *Fractal Concepts in Surface Growth*, Cambridge University Press, Cambridge, MA (1995).
23. T. Nagatani. *Phys. Rev. A* **45**, 2480 (1992).
24. P. Meakin, T. Jossang, J. Feder. *Phys. Rev. E* **48**, 2906 (1993).
25. C. Vautrin-Ul, A. Chausse, J. Stafiej, J. P. Badiali. *Pol. J. Chem.* **78**, 1795 (2004).
26. F. D. A. A. Reis, J. Stafiej, J. P. Badiali. *J. Phys. Chem. B* **110**, 17554 (2006).
27. C. Vautrin-Ul, H. Mendy, A. Taleb, A. Chaussé, J. Stafiej, J. P. Badiali. *Corros. Sci.* **50**, 2149 (2008).
28. D. di Caprio, J. Stafiej. *Electrochim. Acta* **55**, 3884 (2010).
29. D. di Caprio, J. Stafiej. *Electrochim. Acta* **56**, 3963 (2011).
30. L. Stanton, A. Golovin. *Phys. Rev. B* **79**, 035414 (2009).
31. G. Contreras, S. Goidanich, S. Maggi, C. Piccardi, M. V. Diamanti, M. P. Pedeferri, L. Lazzari. *Corros. Rev*. **29**, 241 (2011).
32. S. V. Lishchuk, R. Akid, K. Worden, J. Michalski. *Corros. Sci.* **53**, 2518 (2011).
33. N. J. Laycock, S. P. White. *J. Electrochem. Soc*. **148**, 8264 (2001).
34. D. E. Williams, M. L. Kilburn, J. Cliff, G. I. N. Waterhouse. *Corros. Sci*. **52**, 3702 (2010).
35. F. D. A. A. Reis, J. Stafiej. *Phys. Rev. E* **76**, 011512 (2007).
36. F. D. A. A. Reis, J. Stafiej. *J. Phys.: Condens. Mater.* **19**, 065125 (2007).
37. W. Chmielewski, D. di Caprio, J. Stafiej. *Proceedings of the International Conference on Scientific Computing* (CSC'11), L. D'Alotto, J. F. Nystrom, A. M. G. Solo, W. Spataro (Eds.), pp. 236–240 (2011).

